Asia-Pac. J. Atmos. Sci., 51(3), 275-290, 2015
DOI:10.1007/s13143-015-0077-2
pISSN 1976-7633 / eISSN 1976-7951

Effects of Mountain Uplift on Global Monsoon Precipitation

June-Yi Lee[1], Bin Wang[2,3], Kyong-Hwan Seo[1,4], Kyung-Ja Ha[1,4], Akio Kitoh[5], and Jian Liu[6,7]

[1]*Research Center for Climate Sciences, Pusan National University, Busan, Korea*
[2]*International Pacific Research Center and Department of Meteorology, University of Hawaii, Honolulu, U.S.A.*
[3]*Earth System Modeling Center, Nanjing University of Information Science and Technology, Nanjing, China*
[4]*Department of Atmospheric Sciences, Pusan National University, Busan, Korea*
[5]*University of Tsukuba, Tsukuba, Japan*
[6]*Key Laboratories for Virtual Geographic Environment and Numerical Simulation of Large Scale Complex System, School of Geography Science, Nanjing Normal University, Nanjing, China*
[7]*Jiangsu Center for Collaborative Innovation in Geographical Information Resource Development and Application, Nanjing 210023, China*

(Manuscript received 9 March 2015; accepted 3 August 2015)

Abstract: This study explores the role of the global mountain uplift (MU), which occurred during the middle and late Cenozoic, in modulating global monsoon precipitation using the Meteorological Research Institute atmosphere-ocean coupled model experiments. First, the MU causes changes in the annual mean of major monsoon precipitation. Although the annual mean precipitation over the entire globe remains about the same from the no-mountain experiment (MU0) to the realistic MU (MU1), that over the Asian-Australian monsoon region and Americas increases by about 16% and 9%, respectively. Second, the MU plays an essential role in advancing seasonal march, and summer-monsoon onset, especially in the Northern Hemisphere, by shaping pre-monsoon circulation. The rainy seasons are lengthened as a result of the earlier onset of the summer monsoon since the monsoon retreat is not sensitive to the MU. The East Asian monsoon is a unique consequence of the MU, while other monsoons are attributed primarily to land-sea distribution. Third, the strength of the global monsoon is shown to be substantially affected by the MU. In particular, the second annual cycle (AC) mode of global precipitation (the spring-autumn asymmetry mode) is more sensitive to the progressive MU than the first mode of the AC (the solstice mode), suggesting that the MU may have a greater impact during transition seasons than solstice seasons. Finally, the MU strongly modulates interannual variation in global monsoon precipitation in relation to El Niño and Southern Oscillation (ENSO). The Progressive MU changes not only the spatial distribution but also the periodicity of the first and second AC mode of global precipitation on interannual timescale.

Key words: Mountain uplift, global monsoon precipitation, Asian-Australian monsoon, coupled model experiment, ENSO-global monsoon relationship

1. Introduction

The tectonic uplift of the Tibetan Plateau (TP), the Himalayas, and the plateaus of the American west occurred on a large scale and at an accelerating rate (Ruddiman and Kutzbach, 1989; Sepulchre et al., 2006) during the middle and late Cenozoic, i.e., 20 to 50 million years (Ma) ago. The land-sea distribution has remained more or less the same since then except for the 200-km widening of the Atlantic Ocean in the last 10 Ma (Barron et al., 1981). By conducting experiments using atmospheric general circulation models with and without the mountain uplift (MU), it has been demonstrated that the MU interrupted the more zonally oriented atmospheric circulation in the earlier Cenozoic and increased the "continentality" of climate, leading to features such as greater east-west differentiation, colder winters, and more uneven seasonal precipitation in the Northern Hemisphere (Manabe and Terpstra, 1974; Barron, 1985; Rudiman and Raymo, 1988; Ruddiman and Kutzbach, 1989; and many others).

Recent studies have suggested that the climate system response to the MU may be much stronger in a coupled atmosphere-ocean model than in an atmosphere-only model (Abe et al., 2004; Kitoh, 2004; Okajima and Xie, 2007). From the Meteorological Research Institute global ocean-atmosphere coupled GCM (MRI-CGCM) experiments with the progressive MU, Abe et al. (2004) showed that the MU not only modifies atmospheric circulation and precipitation, but also plays a crucial role in the evolution of the tropical coupled atmosphere-ocean system over the Indian and Pacific Oceans. Kitoh (1997, 2002, 2007, 2010) used the MRI-CGCM experiments to further demonstrate that the MU causes changes in ocean circulation and sea surface temperature (SST), and regulates the intensity and period of El Niño and Southern Oscillation (ENSO). Okajima and Xie (2007) showed that the Western North Pacific (WNP) climate is affected by orography through wind-evaporation-SST feedback.

It has been recognized that the TP and Himalayas serve as either elevated heat sources or orographic insulators that drive the gigantic Asian summer monsoon (ASM) system (Kutzbach et al., 1989; Kitoh, 2002, 2004, 2010; Liu and Yin, 2002; Abe et al., 2003, 2004; Yasunari et al., 2006; Wu et al., 2007; Boos and Kuang, 2010). Abe et al. (2004) and Kitoh (2004, 2010) demonstrated that owing to the thermal and barrier effects of

Corresponding Author: Kyong-Hwan Seo, Department of Atmospheric Sciences, Pusan National University, San 30, JangjeonDong, Geumjeong-Gu, Busan 609-735, Korea.
Email: khseo@pusan.ac.kr

the MU, precipitation areas tend to shift inland over the Asian continent, and the North Pacific subtropical anticyclone and southwesterly monsoon flows that transport abundant moisture toward East Asia are both enhanced. Using an atmospheric model, Liu and Yin (2002) suggested that the East Asian monsoon is more sensitive to the uplift of the TP than the South Asian monsoon is. Recently, Boos and Kuang (2010) demonstrated that the narrow orography of the Himalayas and adjacent mountain ranges can produce a strong South Asian monsoon by insulating the warm, moist air over continental India from the cold and dry air of the extratropics.

Over the past decade, the concept of global monsoon has been established as a global-scale, persistent atmospheric overturning circulation system that varies according to the time of year (Trenberth et al., 2000, 2006; Trenberth and Stepaniak, 2004) and as a response of the coupled atmosphere-land-ocean system to the annual variation in solar forcing (Wang and Ding, 2008). Understanding the annual variation in global monsoon precipitation is of importance because the monsoon precipitation plays an essential role in determining Earth's general circulation and hydrological cycle. Wang and Ding (2008) proposed that the primary climatological features of the global monsoon can be represented by three-parameter metrics: the annual mean and two major modes of the annual variation in the global monsoon, namely, a solstitial mode and an equinoctial asymmetric mode. These metrics have been proven to be a very useful tool for gauging the performance of current models in simulating the annual variation in global monsoon precipitation (Lee et al., 2010; Kim et al., 2011; Wang et al., 2011; Lee and Wang 2014). The metrics are also applicable to studies on the centennial variation of monsoon precipitation in the last millennium using a coupled ocean-atmosphere model (Liu et al., 2009, 2012) and modern dynamics (Wang et al., 2012).

In contrast to many previous studies that address the impacts of the MU on Asian summer and winter monsoon, this study explores the influence of the global MU on the global monsoon system and its annual variation by analyzing a series of MRI-CGCM experiments using varying mountain heights. This is to take into account the fact that the three-parameter global monsoon metrics can articulate a global linkages among regional monsoons, thus providing a better understanding of mechanisms and characteristics of their climatological annual variation. This study is of significance for understanding the mechanisms of global monsoon because the MU is one of the important external forces affecting global monsoon variations on a geological timescale. In section 2, the MRI-CGCM and experimental design are described. In section 3, the impact of the MU on annual and seasonal mean precipitation and global atmospheric circulation is discussed. Section 4 describes the annual cycle of regional monsoon precipitation over the eight monsoon sub-domains. In section 5, the influence of progressive MU on the global monsoon system is discussed in terms of the three-parameter metrics and global monsoon precipitation domain. Section 6 investigates how the progressive MU modulates interannual variation in global monsoon precipitation in relation with ENSO. In the last section, the major findings are summarized and limitations of this study are discussed.

2. Description of model and experimental design

The model used in this study is MRI-CGCM version 2.2.2, and it includes the Japan Meteorological Agency atmospheric model and a Bryan-Cox ocean model (Kitoh, 2007). The horizontal resolution of the atmospheric model is T42 in wave truncation and the vertical configuration consists of a 30-layer sigma-pressure hybrid coordinate. The horizontal grid spacing of the ocean model is 2.5° in longitude and 2.0° in latitude. Between 4°S and 4°N, the meridional grid spacing is reduced to 0.5° in order to resolve the equatorial oceanic waves adequately.

In this study, we analyze orography sensitivity experiment data, which were used in Abe et al. (2004), Kitoh (2004, 2007), and Kitoh et al. (2010). There were eight runs with MU of 0 (MU0: no mountain), 0.2, 0.4, 0.6, 0.8, 1 (MU1: control run), 1.2, and 1.4 times the height of the observed mountains. The same land-sea distribution was used in all experiments and global mountain heights were uniformly varied. In the case of the MU0 run, a realistic land-sea distribution is preserved but with zero height for all mountains. Figure 2 of Abe et al. (2003) shows the global orography used for the control run (MU1). The top elevation of the TP is 4,400 m. All experiments were free coupled runs and were integrated for 50 years with the same initial condition (January 1st) from the flux-adjusted run of the same coupled model (Yukimoto et al., 2001). The data only for the last 30 years were used to determine the monthly climatology in order to prevent errors introduced by a climate drift. It should be mentioned that the smoothing of the spectral representation of the model's orography is inevitable and that narrow mountain ranges, such as the Himalayan Ranges and the Burmese Mountains, are not well resolved. Therefore, this may underestimate circulation response to the MU.

MRI-CGCM version 2.2.2 is capable of reproducing the observed seasonal climatology of precipitation and SST in the case of MU1. However, as described in Kitoh (2004), it has systematic biases that may, in part, compromise interpretation of the experimental results. First, a double intertropical convergence zone (ITCZ) is obvious in the coupled model, associated with low SSTs and suppressed precipitation along the equatorial Pacific, especially during March-April-May (MAM) and December-January-February (DJF). In addition, the model particularly overestimates the strength of the South Pacific convergence zone (SPCZ). Second, a significant warm bias along with abundant precipitation is observed over the subtropical eastern Pacific in both the Northern and Southern Hemispheres for all seasons. Third, precipitation over the Maritime Continent (MC), the TP, the Rockies, and the Andes for all seasons tends to be overestimated. The excessive precipitation over the TP is one of common biases in the current global climate models. Su et al. (2013) found that CGCMs in the phase 5 of Coupled Model Intercomparison Project

simulate excessive precipitation over the TP by 60-180%. Finally, warm SST biases are observed over the Indian Ocean and the South Atlantic in all seasons.

The present-day observed climatology data used for verification were obtained from the Climate Prediction Center Merged Analysis of Precipitation data set (Xie and Arkin, 1997) and from the improved Extended Reconstructed Sea Surface Temperature Version 2 (ERSST V2) data (Smith and Reynolds, 2004) for the 31 years between 1979 and 2009.

3. Effects of the MU on annual and seasonal mean climates

We first investigate the effects of the MU on annual and seasonal (solstitial and transitional) mean climates over the entire globe by comparing MU1 and MU0 results. Solstice

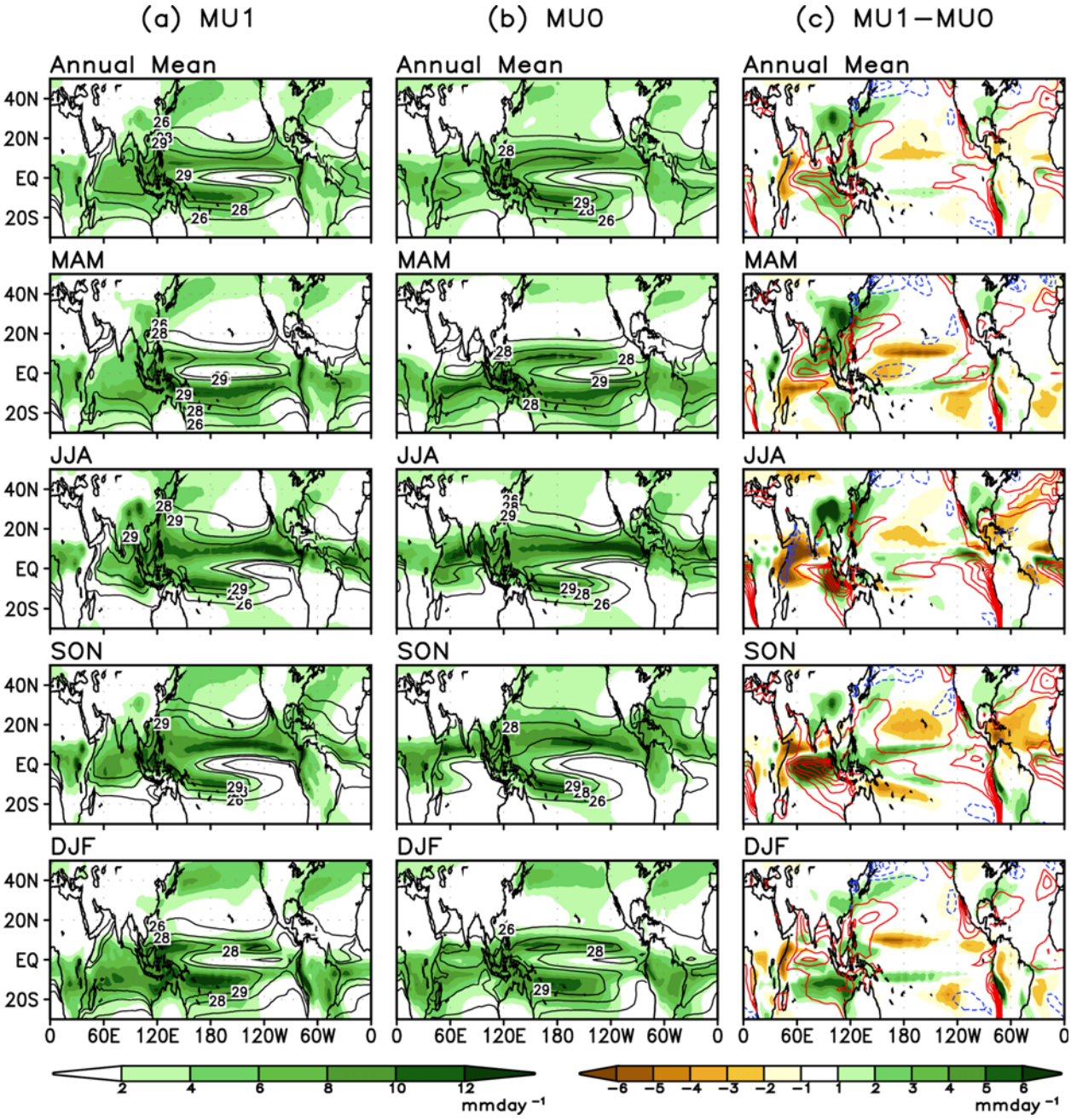

Fig. 1. Geographical distributions of climatological annual mean and seasonal mean of precipitation (shading) and SST (contour) reproduced by the (a) MU1 (control) and (b) MU0 (no-mountain) experiments, respectively. (c) Difference between the precipitation and SST of the MU1 experiment and those of MU0 experiment. The unit for precipitation is mm day^{-1}. Contour levels of SST in (a) and (b) are 26, 28, and 29°C. The contour interval of SST in (c) is 1°C. In (c), differences exceeding a *t*-test at the 95% confidence interval are exhibited.

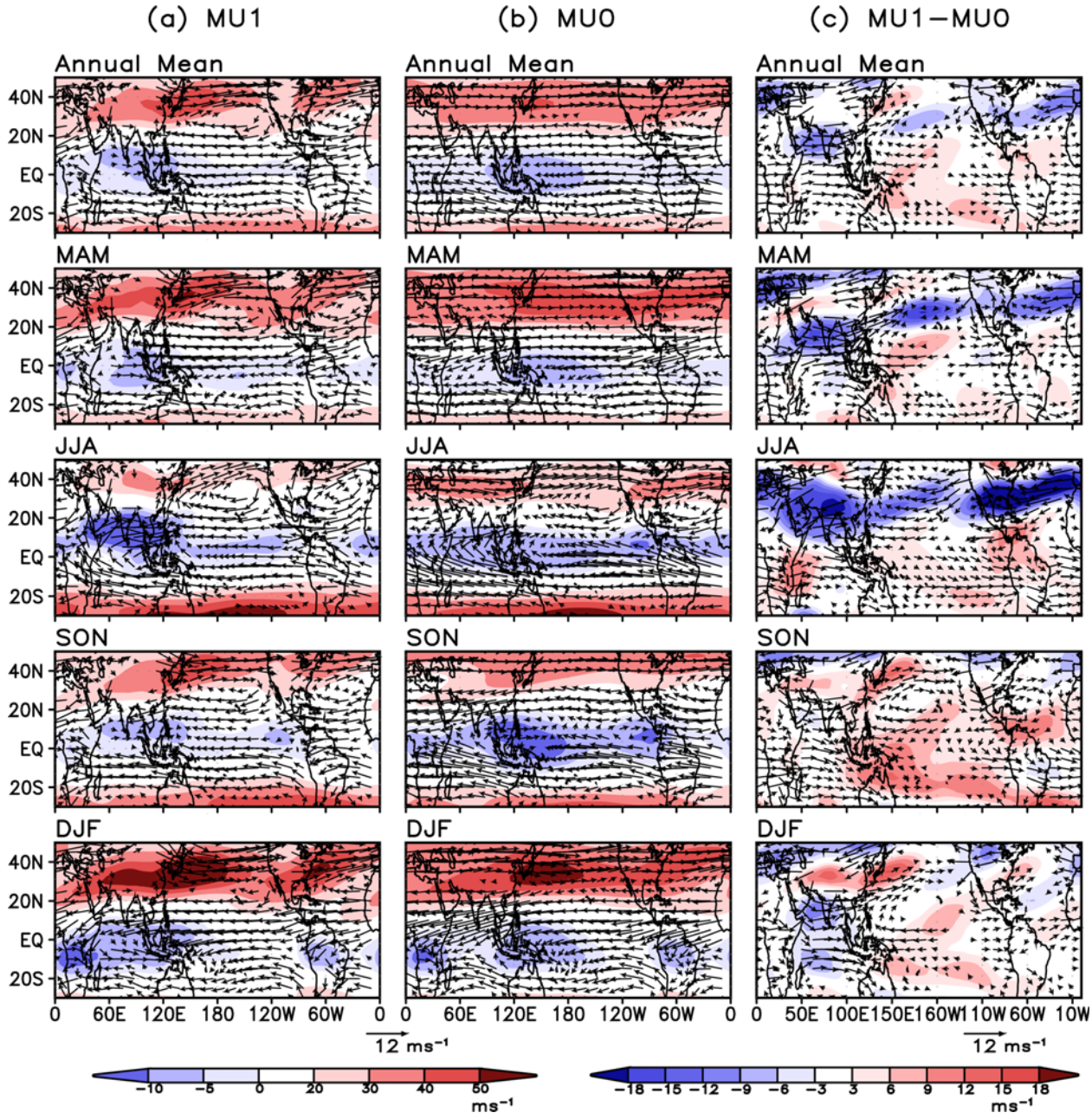

Fig. 2. Same as Fig. 1, except for 200 hPa zonal wind (shading) and 850 hPa wind (vector). The unit for wind is m s^{-1}.

seasons include June-July-August (JJA) and DJF, and transition seasons include MAM and September-October-November (SON). Since considerable effort has been devoted to exploring the impact of the MU on Asian summer- and winter-monsoon climates (e.g., Kitoh, 2002, 2004, 2010; Liu and Yin, 2002; Abe et al., 2003, 2004, 2005; Lee et al., 2013), particular attention is paid to the effects of the MU on annual mean and transition season mean climates on a global scale.

Significant differences in the annual and seasonal means of precipitation, atmospheric circulation, and SST between MU0 and MU1 are observed over the regions not only proximal to but also remote from the uplifted terrains (Figs. 1 and 2). In particular, the Asian-Australian monsoon (A-AM) system exhibits a drastic alteration in all seasons as a result of the MU. The climatological annual mean precipitation over the A-AM region (30°S-40°N, 40°-160°E) increases by about 16% from MU0 (3.70 mm day^{-1}) to MU1 (4.29 mm day^{-1}), while that over the entire globe remains about the same with a slight decrease (2.94 mm day^{-1} for MU0 and 2.92 mm day^{-1} for MU1) as shown in Fig. 3. Annual mean precipitation over Americas (land only region over 30°S-40°N, 120°-30°W) also increases by about 9% but that over Africa (land only region over 30°S-40°N, 30°W-60°E) decreases by about 10% from MU0 to MU1. Precipitation decrease with the realistic MU is

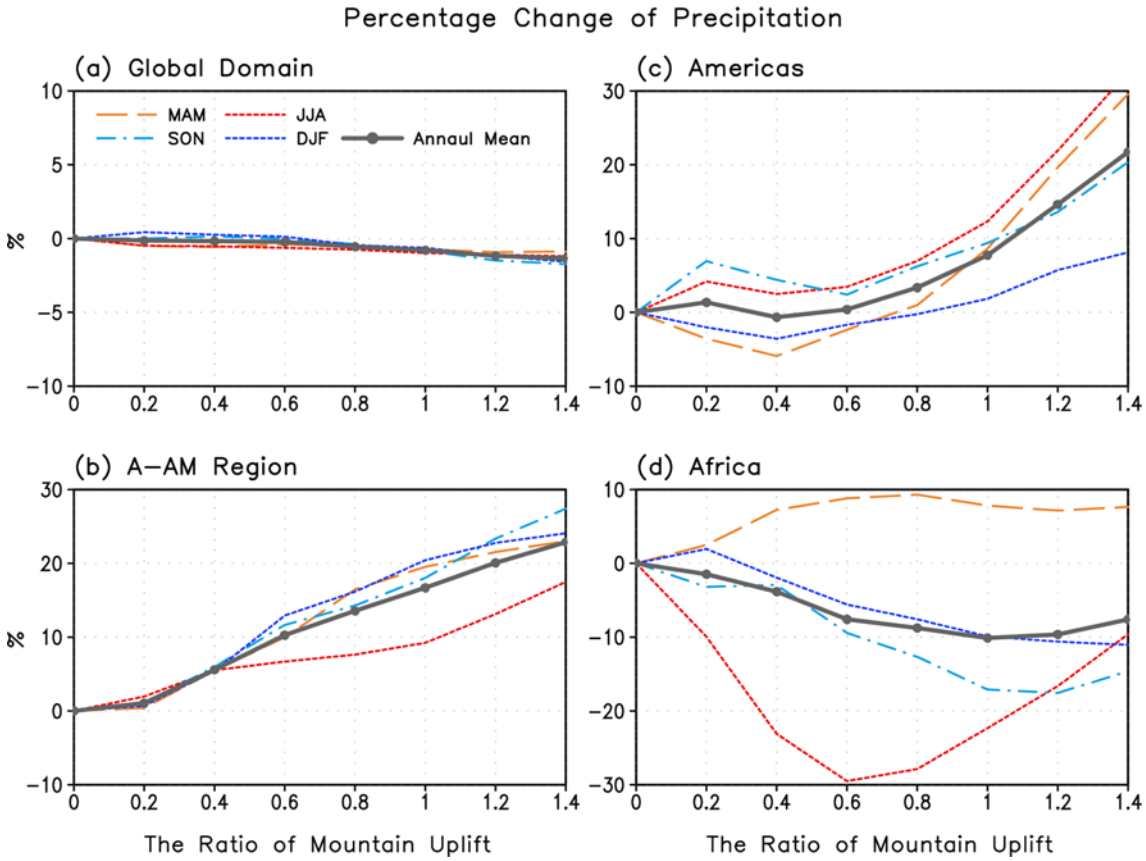

Fig. 3. Percentage change of precipitation against the MU0 experiment as a function of the MU ratio from zero to 1.4 averaged over (a) the global domain, (b) the entire A-AM region (30°S-40°N, 40°-160°E), (c) Americas (land only over 30°S-40°N, 120°-30°W) (d) Africa (land only over 30°S-40°N, 30°W-60°E).

mainly observed over the subtropical Pacific and Atlantic and Western Indian Ocean.

The MU-induced changes in the annual mean climate are notable over the following four regions: (1) high-elevated terrains, (2) the Indian Ocean, (3) East Asia and its adjacent seaboard, and (4) Eastern North America and its adjacent seaboard. Their properties are summarized as follows: first, the mechanical and thermal effects of the MU cause a direct increase in the precipitation over the TP, Sierra Madre, and the Andes. Second, the MU causes an increase in the precipitation in the eastern Indian Ocean possibly via the SST increase and low-level convergence due to weakening of the South Indian Ocean trade wind and enhancement of cyclonic circulation. However, the MU simultaneously results in a reduction of the precipitation in the western Indian Ocean possibly via SST decrease due to enhanced cross-equatorial flow-induced upwelling and evaporation. Third, the MU causes the rearrangement of the atmospheric flow from being nearly zonal in the case of MU0 to meandering in MU1, resulting in the considerable intensification of low-level subtropical anticyclones over the North Pacific and North Atlantic. It also increases precipitation over East Asia, eastern North America and their adjacent seaboards. In particular, the MU causes an increase in the SST over the equatorial eastern Indian Ocean and the weakening of the Pacific cold tongue particularly during northern summer and fall. This is related to the weakening of the Southern Hemisphere trade winds and deepening of the thermocline. However, the process by which the MU weakens the southeast trades over the Southern Hemisphere is not yet clearly understood.

The MU-induced changes in transition seasons are as large as those in solstice seasons (Figs. 1c, 2c, and 3b-d). In MAM, the MU considerably enhanced precipitation over East Asia in concert with the formation of the strong North Pacific anticyclonic circulation and SST warming over the North Indian Ocean and the WNP. The SST warming is associated with the weakening of easterly basic flow in the lower troposphere, which results from the MU-induced cyclonic circulation over southeastern Asia. Similar effects were seen over eastern North America and the western North Atlantic. These results indicate that the MU affects the pre-monsoon circulation and precipitation, and thus ante dates the seasonal march and summer-monsoon onset over the Asian monsoon region and eastern North America. The MU's impacts on seasonal march and monsoon onset will be revisited in section 4. Enhanced precipitation during boreal spring over mid-latitude East Asia, eastern North America, the North Pacific, and the North Atlantic is attributable in part to considerable

synoptic disturbance activity when mountains exist (Broccoli and Manabe, 1992; Lee et al., 2013).

In SON, the most striking difference between the two experiments is observed over the Tropical Indian Ocean. In MU0, strong low-level easterly winds prevail over the subtropical South and North Indian Ocean, thus increasing precipitation and SST over the Western Indian Ocean and decreasing them over the Eastern Indian Ocean (the second panel from the bottom in Fig. 1b). However, mountains with realistic heights (MU1) reduce the easterly flow over the subtropical region and enrich precipitation along with large SST warming over the equatorial and South Indian Ocean (the second panel from the bottom in Fig. 1a). Precipitation over the MC, Indian subcontinent, and central China increases. The anticyclonic circulation over the North Pacific and the North Atlantic also strengthens in MU1, resulting in enhanced precipitation over the WNP, eastern North America, and the parts of the Atlantic Ocean adjacent to eastern North America.

As indicated in the results of previous studies (e.g., Abe et al., 2003; Kitoh 2004), the strong thermal contrast and barrier effects of the MU strongly intensify the southwest monsoon over the North Indian Ocean and the anticyclonic circulation over the North Pacific in JJA, supplying warm, moist air to the Asian monsoon region. It is observed that the monsoon trough can form in the absence of the MU over the subtropical ocean, but the uplift pushes the monsoonal trough northwestward in Asia and the North Pacific. A similar MU effect is also found over eastern North America and the North Atlantic. In DJF, the MU increases the austral summer-monsoon precipitation over the MC and the South Indian Ocean convergence zone. Storm track activities are strengthened with the MU over East Asia-WNP and eastern North America, in addition to the intensification and southwestward shift of jet streams similar to the results shown in Lee et al. (2013). Park et al. (2013) suggested that the southward shift of the jet is attributable to the TP-induced winter stationary waves.

4. Analysis of regional monsoon components

In this section, we examine how the seasonal march of regional monsoon precipitation is modulated by progressive MU in the MRI-CGCM. This takes into account distinctive regional characteristics of the global monsoon system. While previous studies have focused mainly on the Asian monsoon system and the Western North Pacific climate, the current investigation has been broadened into eight regional monsoon components: the East Asian monsoon (EAM, 20°N-40°N, 100°E-140°E), Indian monsoon (IM, 5°N-30°N, 65°E-105°E), WNP monsoon (WNPM, 10°N-22.5°N, 105°E-160°E), Australian monsoon (5°S-20°S, 105°E-160°E), North American monsoon (5°N-22.5°N, 110°W-80°W), South American monsoon (5°S-25°S, 75°W-40°W), West African monsoon (2.5°N-15°N, 20°W-40°E), and South African monsoon (5°S-25°S, 10°E-80°E).

Figure 4 shows the annual cycle (AC) of the regional precipitation in the eight monsoon sub-domains in the observation and coupled experiments with progressive MU. The MU plays a significant role in determining the phase and amplitude of the precipitation AC in regional sub-monsoon systems, particularly in the four regional components of the A-AM system (Figs. 4a-d). The spread of the AC lines for the varying MU indicates that the EAM is the most sensitive to the progressive MU (Fig. 4a). The EAM is a unique consequence of the MU, while other monsoons owe their presence primarily to the realistic land-sea distribution. The progressive MU advances the EAM's onset and prolongs the summer-monsoon period, with an approximately linear response. The amount of summer mean precipitation over the EAM region increases by 74% and the amplitude (or strength) of the annual cycle is enhanced by 50% from MU0 to MU1.

The IM is also significantly modulated by the MU (Fig. 4b). The progressive MU accelerates the onset of the IM and increases the amplitude systematically up to MU1.4. The MU has less impact on the retreat of the IM. The onset is advanced by about one month from MU0 to MU1. MU1 captures the most realistic AC. However, the model inherently underestimates precipitation intensity. In contrast to the IM, the phase of the WNPM's AC is more significantly modulated by the progressive MU (onset advanced by two months) but its amplitude is not affected (Fig. 4c). WNPM's onset tends to be gradually advanced from MU0 to MU0.8 but delayed afterward. The model with the realistic mountain height fails to simulate an August peak in the WNP. Lee et al. (2010) found that the failure in capturing the August peak of the WNP precipitation is one of common biases in the current coupled models.

In spite of the fact that the Australian monsoon is located remotely from the major uplifted terrains, the progressive MU systematically enhances austral summer rainfall and prolongs its rainy period (Fig. 4d). The model intrinsically overestimates the AC's amplitude and the austral rainy period. The model's overestimation of the austral monsoon precipitation may be related to the warm SST bias along the west coast of Australia and the excessive moisture convergence over the Australian monsoon region.

The MU in the American west encompassing the Sierras and Rockies, the Colorado Plateau, and the Andes plays an important role in regulating the North American and South American monsoon precipitation. From MU0 to MU1.4, the progressive MU is observed to advance the onset (retreat) of the North American monsoon by about one month (half month, respectively), and enhance the amount of summer-monsoon rainfall (Fig. 4e). Because the coupled model intrinsically underestimates precipitation during the first half of the rainy season and overestimates it during the second half with the realistic MU, MU1.4 captures the AC of the North American monsoon precipitation more realistically than other runs. The existence of the MU advances the onset of the South American monsoon by about half a month and enhances summer precipitation. Overall, the MU has the least impact on the South American monsoon among all regional monsoons (Fig. 4f).

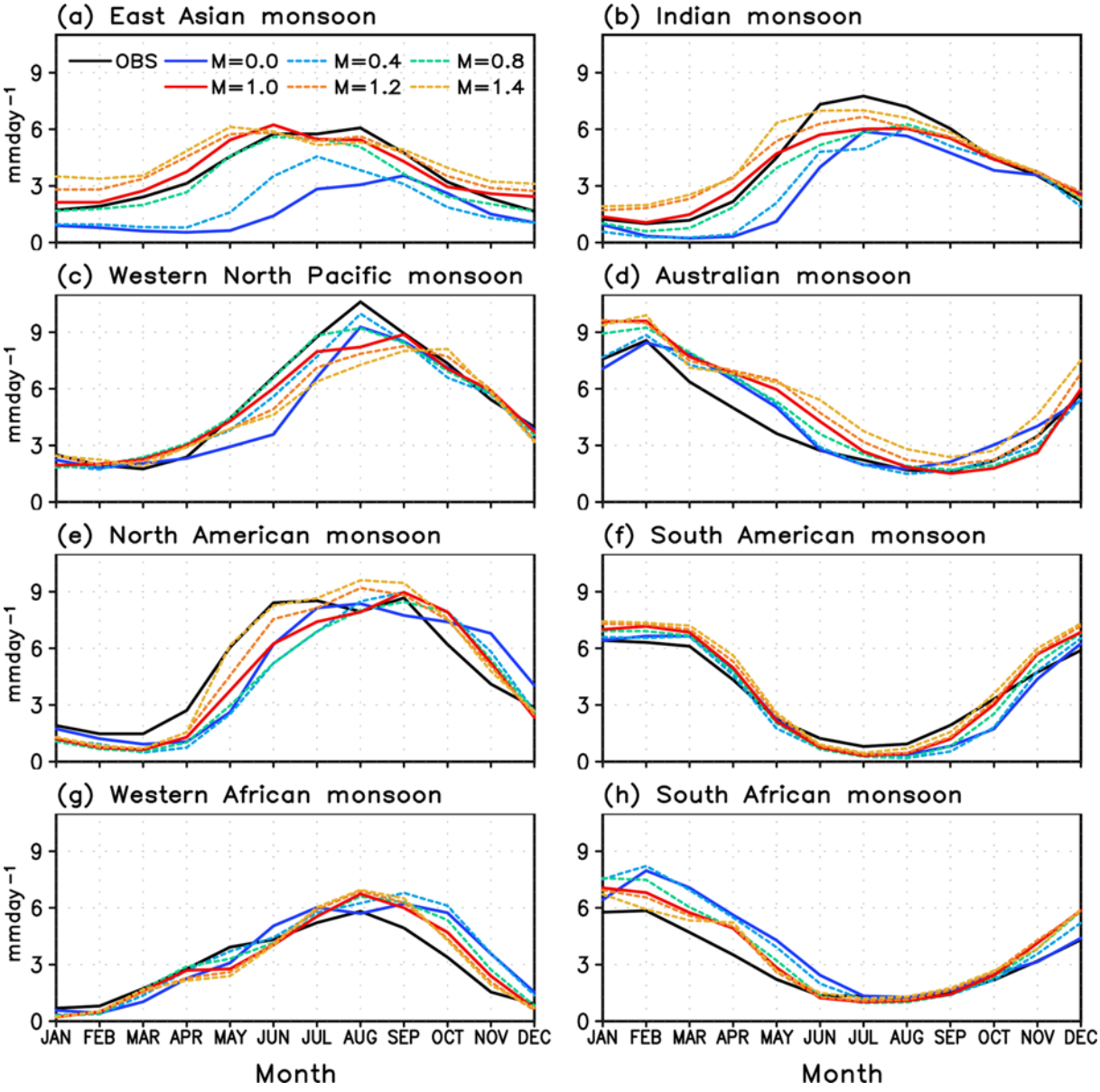

Fig. 4. The annual cycle of precipitation in (a) East Asia (20°-40°N, 100°-140°E), (b) Indian (5°-30°N, 65°-105°E), (c) Western North Pacific (10°-22.5°N, 105°-160°E), (d) Australian (5°-20°S, 105°-160°E), (e) North American (5°-22.5°N, 110°-80°W), (f) South American (5°-25°S, 75°-40°W), (g) Western African (2.5°-15°N, 20°W-40°E), and (h) South African (5°-25°S, 10°-80°E) monsoon region, respectively, obtained from the observation and the model simulations with the progressive MU ratio from zero to 1.4.

The uplift-induced changes in the AC of the Western African and South African Monsoon are relatively small (Figs. 4g and h). The progressive MU affects the Western African monsoon precipitation only in the phase of its AC whereas the South African monsoon is affected in both the phase and amplitude of its AC. In particular, the MU advances the retreat of the Western African and South African monsoon by about half a month from MU0 to MU1. In contrast to other regional components, the MU tends to reduce the amplitude of the AC of the South African monsoon, which leads to a decrease in annual mean precipitation over Africa as shown in Fig. 3d.

5. Analysis of global monsoon

Wang and Ding (2008) and Wang et al. (2011) proposed simple metrics for analyzing global monsoon; these include 1) the first and 2) second annual cycle (AC) modes (the solstice and equinox asymmetric mode, respectively), and 3) the monsoon rain domain. The analysis of global monsoon characteristics is of particular importance for understanding the physical processes by which the tropical hydrological cycle and the coupled atmosphere-land-ocean system respond to solar radiative forcing. This section is devoted to investigating the role of the progressive MU on the first two AC modes and

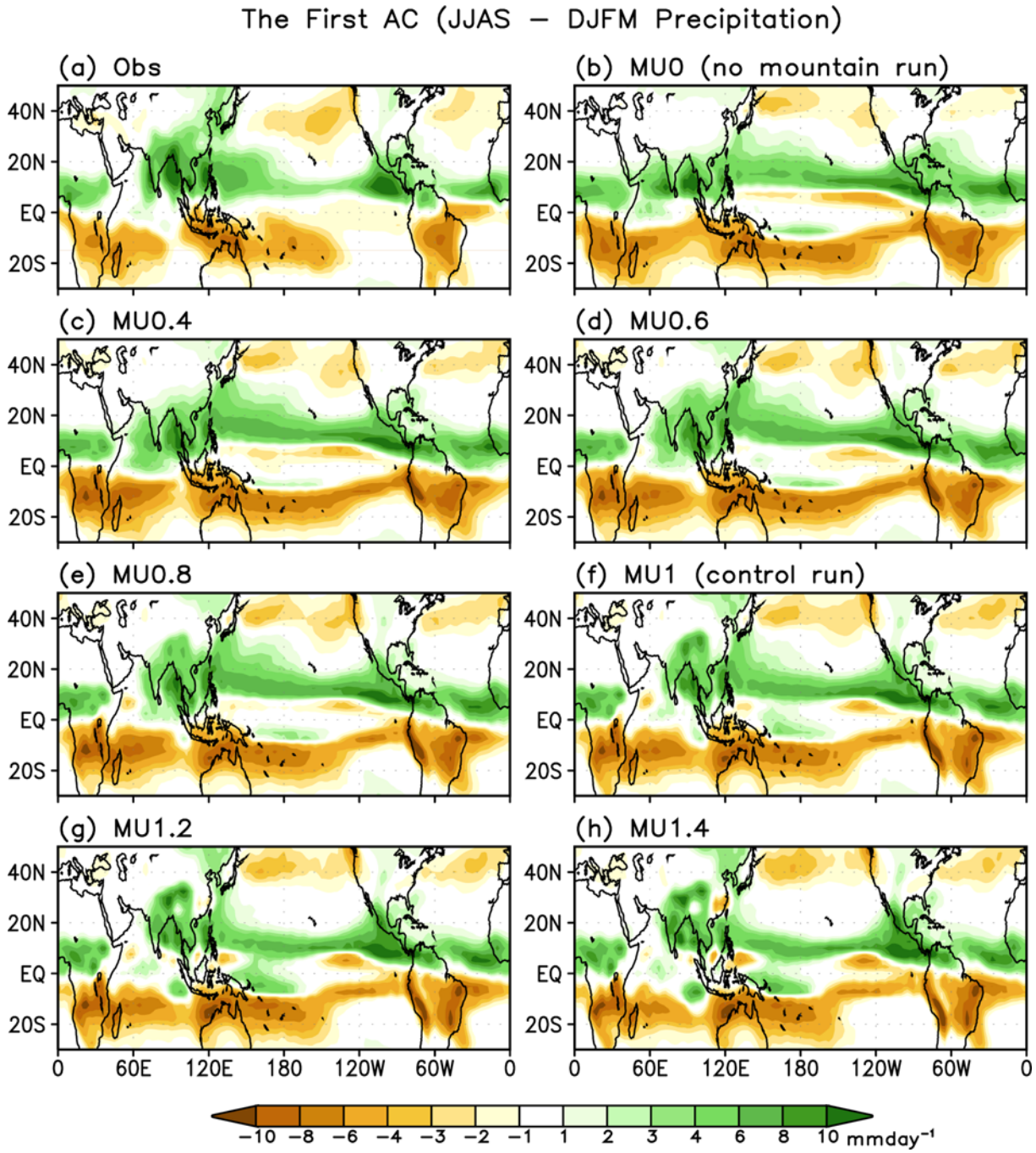

Fig. 5. Spatial pattern of differential precipitation between June-July-August-September and December-January-February-March (JJAS minus DJFM) in (a) the observation and the MRI coupled simulation with the MU ratio varying from (b) 0 to (h) 1.4, respectively. The unit is mm day^{-1}.

the monsoon rain domain.

a. The first AC mode

The first AC mode is depicted by the difference between the mean precipitation of June-July-August-September (JJAS) and that of December-January-February-March (DJFM), which reflects the atmospheric response to solar forcing in the solstice seasons with a one- to two-month phase delay and also measures the annual range of precipitation (Wang et al., 2011). Figure 5 shows the spatial pattern of the first AC mode of precipitation in the observation and coupled experiments with the progressive MU from 0 to 1.4 times the height of the present-day mountains. The coupled model is capable of capturing the observed annual range of precipitation without the MU to some extent, but the precipitation in MU0 is zonally

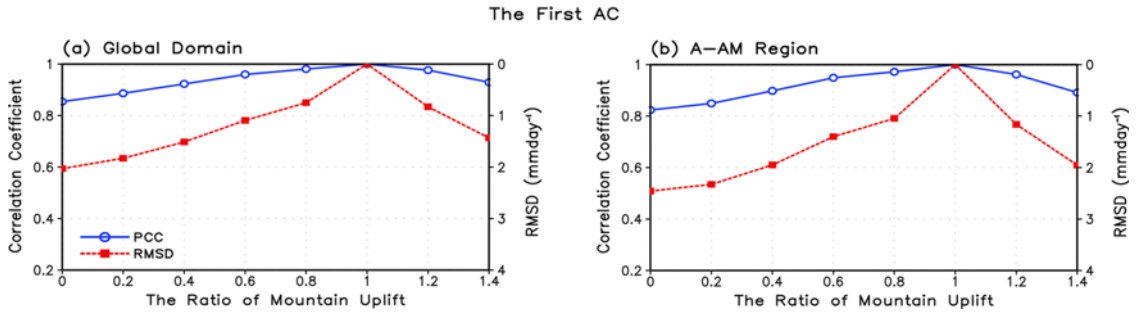

Fig. 6. The pattern correlation coefficient (PCC) and root mean square difference (RMSD) against the MU1 experiment for the first annual cycle mode over the (a) global and (b) A-AM region, respectively, as a function of the MU ratio from zero to 1.4. The y-axis for RMSD is reversed.

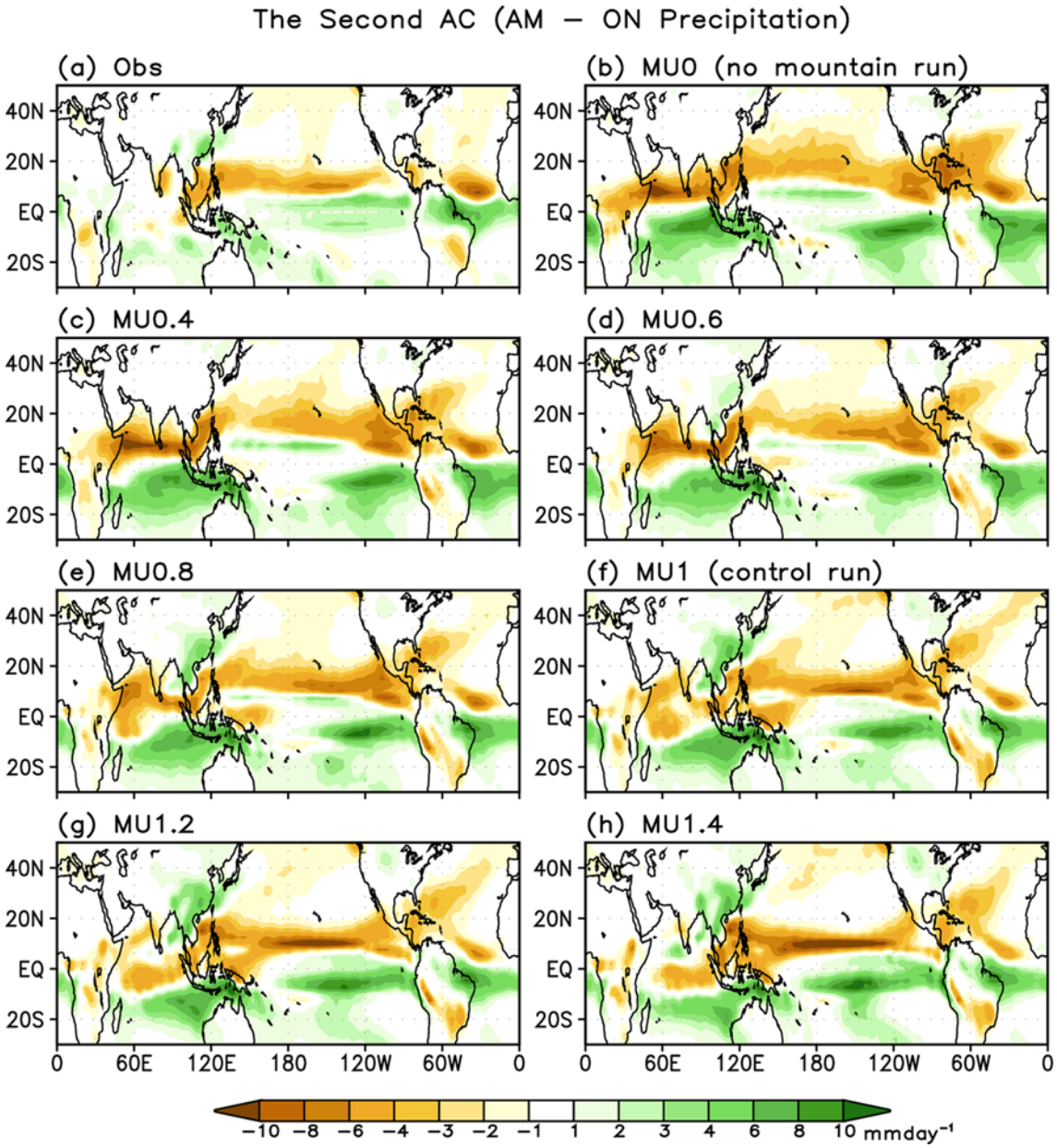

Fig. 7. Same as Fig. 5 except for the second annual cycle mode.

distributed and overestimated in the oceanic regions (Fig. 5b). The progressive MU causes a systematic shift of the monsoon rainfall northward and inland (Figs. 5c-f) toward the observed first AC mode (Fig. 5a). When the MU is exaggerated (MU 1.2 and 1.4 cases), the annual range of precipitation over highly elevated terrains (e.g., the TP and the equatorial sections of the Rockies and Andes) is overestimated and shifted further northward and inland (Figs. 5g-h). In the case of the EAM precipitation, the existence of the MU is essential for forming its solstice monsoon mode, supporting previous studies (Hahn and Manabe, 1975; Ose, 1998; Abe et al., 2004; Kitoh, 2004).

The sensitivity of the first AC mode to progressive MU is depicted in terms of pattern correlation coefficient (PCC) and root mean square difference (RMSD) between MU1 and other experiments over the global and A-AM region, respectively (Fig. 6). The PCC (RMSD) between MU1 and MU0 is 0.84 (2 mm day^{-1}) over the global domain and becomes gradually closer to 1 (0 mm day^{-1}) as mountain height increases up to the height of the present-day mountains. Figure 6 further indicates that the solstice monsoon mode is more sensitive to the progressive MU over the A-AM region than the global region, particularly in terms of RMSD.

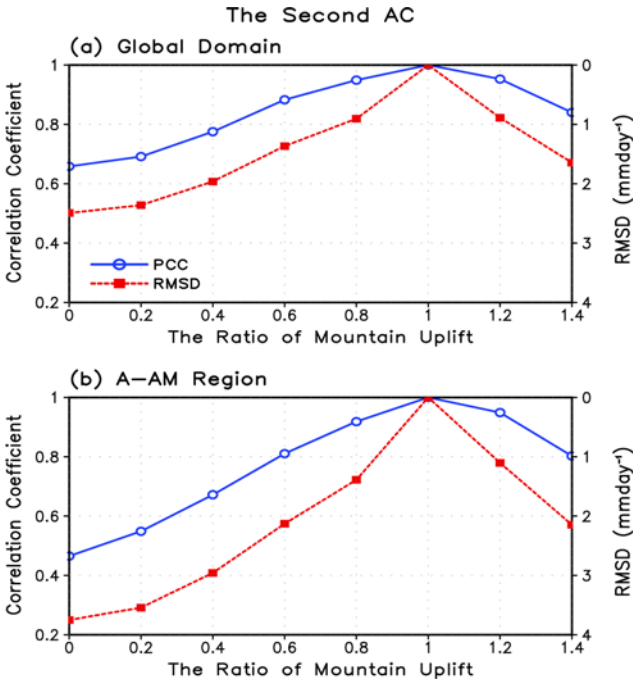

Fig. 8. Same as Fig. 6 except for the second annual cycle mode.

b. The second AC mode

The observed second AC mode shows annual variation with the maximum in April and minimum in October; it represents an asymmetric pattern between the two transitional seasons—the spring-fall asymmetry (Wang and Ding, 2008). The spring-fall asymmetry is one of the fundamental features of the seasonal variation in the tropical circulations; the asymmetry is due to different spatial patterns in the spring and fall ITCZ (Lau and Chan, 1983; Meehl, 1987). The seasonally varying east-west SST gradients may result in the asymmetry over the equatorial Pacific and Indian Oceans (Webster et al., 1998). Chang et al. (2005) suggested that the asymmetry in the A-AM region may be due to the combined effect of asymmetric wind-terrain interaction and low-level divergence induced by different land-ocean thermal inertia.

Figure 7 shows the difference between AM and ON precipitation in the observation and experiments, which represents the second AC mode. Two distinct features are seen in this figure. First, the spring-fall asymmetry seems to prevail over the global tropics without the MU (Fig. 7b), and the progressive MU considerably decreases the asymmetry, particularly over the Indian Ocean (Figs. 7c-h). Second, the MRI-CGCM intrinsically overestimates the asymmetry with the realistic MU over the Indian Ocean (Fig. 7f). Because of the significant systematic error in the MU1, the exaggerated MU tends to help the model to better reproduce the asymmetry (Figs. 7g and h). The SST warm bias over the Indian Ocean (not shown) may be responsible for the CGCM exaggeration of asymmetry over the region of interest but the exact reason for this is still unknown.

A substantially larger sensitivity of the second AC mode to progressive MU than that of the first mode (Fig. 6) is depicted in Fig. 8, which presents the PCC and RMSD for the second mode against the MU1 run. Over the global region (A-AM region), the PCC is 0.62 (0.43) and the RMSD is 2.5 (3.8 mm day^{-1}) between the MU0 and MU1 runs. The remarkable sensitivity of the second AC mode to the progressive MU is likely associated with the advance of season with the existence of the MU shown in Section 4. However, model's systematic bias is a potential factor that may exaggerate the asymmetry.

c. Global monsoon rain domain

The global monsoon rain domain is defined as the regions in which the annual range of precipitation rate exceeds 2 mm day^{-1} and the annual range exceeds 50% of the annual total precipitation (Wang and Ding, 2008). The annual range of precipitation is measured by the local summer-minus-winter precipitation, i.e., MJJAS-NDJFM mean precipitation for the Northern Hemisphere and NDJFM-MJJAS mean precipitation for the Southern Hemisphere.

The simulated global monsoon rain domain with the progressive MU is presented in Fig. 9. The coupled model reasonably reproduces the monsoon rain domain for the no-mountain case except for the EAM region (Fig. 9a), but the simulated domain is nearly zonal. The existence of the MU extends the monsoon domain northward and confines it to the limited region closer to the observed counterpart. Figure 9d also shows that 60% of the present elevation is the threshold value for the formation of the Mei-yu and Baiu rain bands, which is similar to the findings of Kitoh (2004) and Jiang et al. (2008). Using the realistic MU, the coupled model captures the

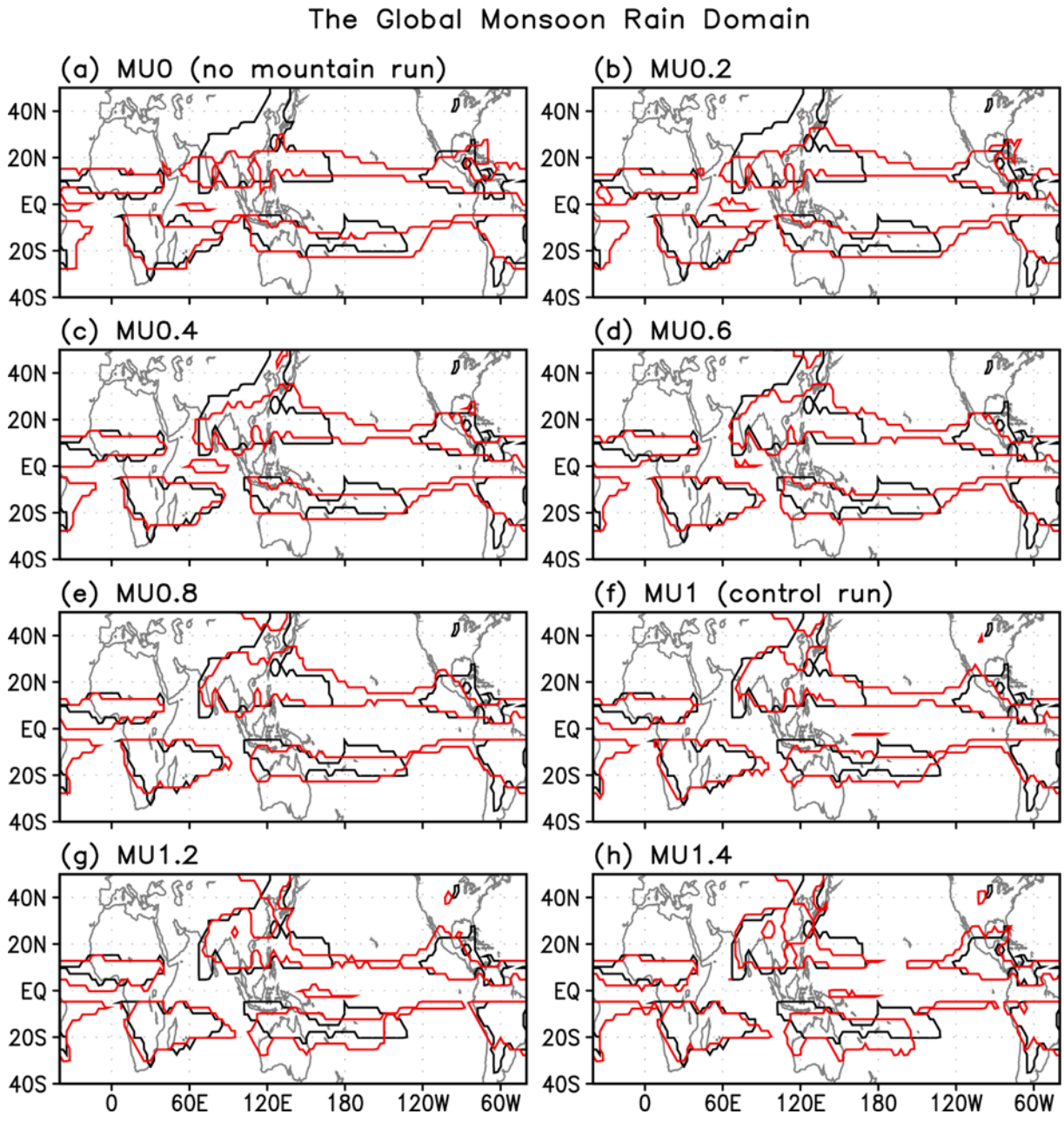

Fig. 9. Global monsoon rain domain derived from the observation (black contour) and the MRI simulations (red contour) with MU ratio of (a) 0 to (f) 1.4.

monsoon rain domain well (Fig. 9f). However, it does not capture the monsoon domain observed over South India, North China and Korea, and it exaggerates the domain over the subtropical Pacific because of its systematic bias. The exaggerated MU further pushes the monsoon domain northward and reduces the domain over the subtropical Pacific (Figs. 9g-h).

To evaluate the similarity between the observed and simulated global monsoon domain, a pattern correlation coefficient and a threat score are calculated. The latter is defined as the number of hit grids divided by the sum of hit, missed, and false-alarm grids (Wang et al., 2011). Figure 10 displays the PCC skill for global monsoon precipitation and monsoon threat score over the observed global monsoon domain as a function of the MU ratio. Two skill measures increase up to the MU ratio of 0.8 and then decrease for the MU ratios higher than 0.8. It is interesting to note that the global monsoon does exist without the mountains but the most realistic distribution is found in the run with the MU of 0.8 times the height of the present-day elevations in the MRI CGCM experiments.

The highest skill for the global monsoon domain with a MU ratio of 0.8 is attributable to the MRI-CGCM's systematic bias with realistic MU conditions: the bias is mainly characterized

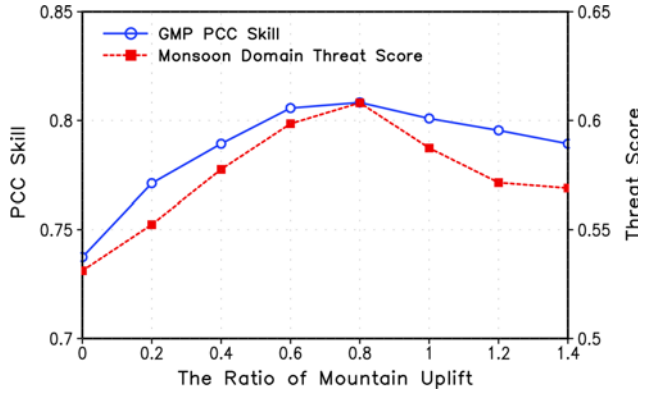

Fig. 10. PCC skill for global monsoon precipitation and monsoon domain threat score as a function of the mountain uplift ratio.

by the underestimation of the Asian monsoon precipitation. The MU1 experiment tends to produce less precipitation over southern China and the WNP, and more precipitation over the TP than MU0, which consequently degrades MU1's simulating skill for global monsoon precipitation. Lee et al. (2010) showed that the state-of-the-art coupled models for seasonal climate prediction have similar systematic bias, although the amplitude of the bias is alleviated by initial conditions.

6. Changes in global monsoon and ENSO relationship

In this section, we examine how the relationship between global monsoon precipitation and ENSO is modulated by progressive MU on interannual timescales. Wang et al. (2012) showed observational evidence of the salient year-to-year interplay between global monsoon precipitation and ENSO. Since ENSO tends to be systematically changed by increases in the height of mountains (Kitoh, 2007), we expect significant modulation of the ENSO-monsoon relationship in the MRI-CGCM experiments. Kitoh (2007) showed that the model ENSO becomes weaker, shorter, and less periodic when mountain height increases.

Empirical orthogonal function (EOF) is applied to the simulated first and second AC mode over the entire globe to identify the leading mode of global monsoon precipitation variability. Figure 11 shows the leading EOF mode of interannual variability of the first AC in the MU0 and MU1 runs. The first EOF mode of the first AC variability accounts for 22.5% of total variance in MU0 and 22.3% in MU1. The MU significantly changes not only the spatial distribution of

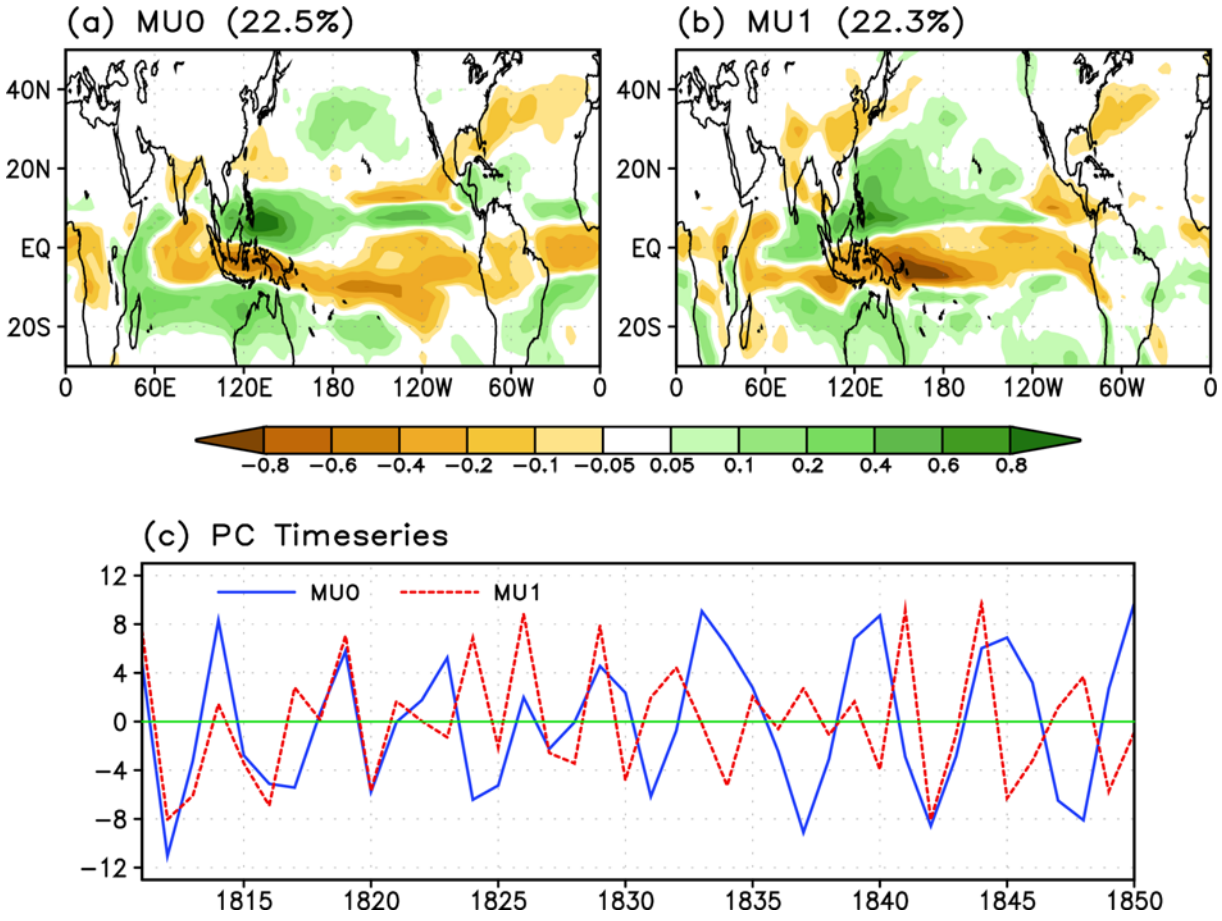

Fig. 11. The spatial patterns of the first EOF eigenvector of the first AC in (a) MU0 and (b) MU1 experiment, and (c) the associated principal components of the first EOF mode for the last 40-year integration.

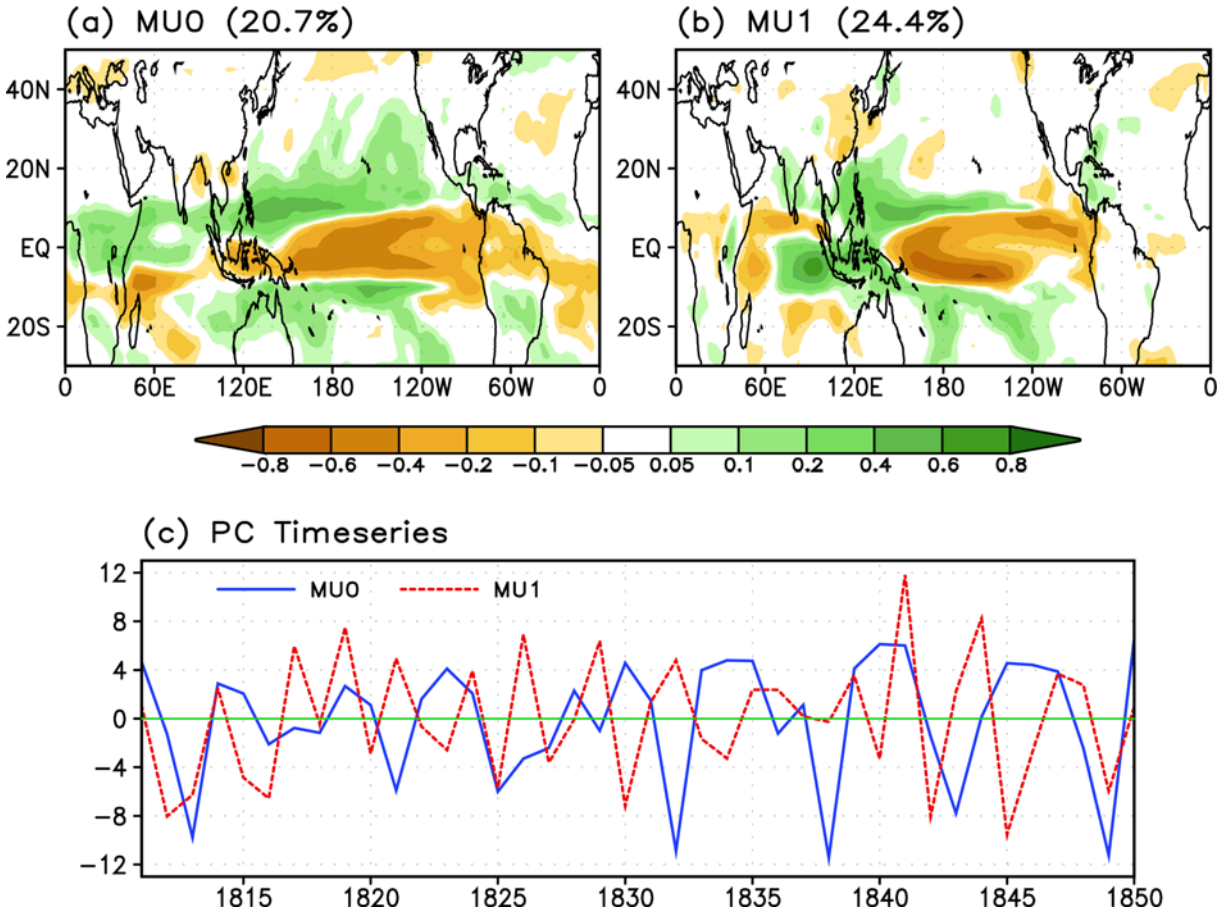

Fig. 12. Same as Fig. 11 except for the second AC.

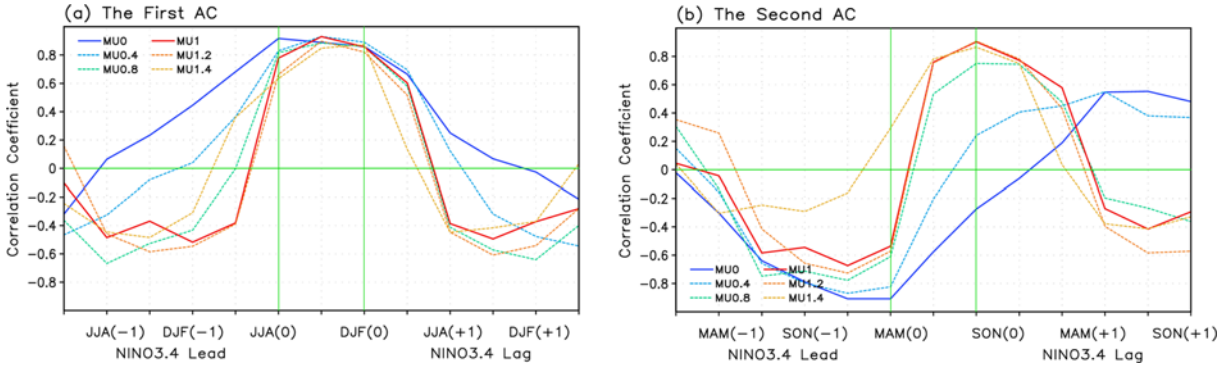

Fig. 13. Lead-lag correlation coefficients of seasonal mean NINO3.4 SST index with reference to the first EOF principal component of (a) the first AC and (b) the second AC simulated by MU experiments.

the leading EOF mode but also the associated temporal variation. The MU tends to strengthen the variability of solstitial asymmetry over the Eastern Hemisphere, particularly the Asian monsoon region, but weaken it over the Western Hemisphere. It is also noted that the first principal component (PC) variation in MU1 is shorter than that in MU0 (Fig. 11c) in relation to changes in ENSO characteristics (Fig. 13a).

Figure 13a indicates that the leading EOF mode of the solstitial asymmetry concurs with ENSO and their relationship is strongly modulated by the progressive MU. Niño 3.4 SST index averaged over 5°S-5°N, 170°-120°W is used to represent ENSO variation. The maximum correlation between the first PC and the seasonal Niño 3.4 SST index does not change from MU0 to MU1 but periodicity of their relationship changes significantly. In MU0, ENSO and its association with global monsoon tend to have 4- to 5-year periodicity while they tend

to have 2- to 3-year periodicity in MU1.

The leading EOF mode of the second AC variability also has a strong relationship with ENSO and is modulated by the progressive MU (Figs. 12 and 13b). The first EOF mode of the second AC variability accounts for 20.7% of total variance in MU0 and 24.4% in MU1. Similar to the solstitial asymmetry shown in Fig. 11, the MU tends to strengthen the variability of equinox asymmetry over the Eastern Hemisphere, in particular, the WNP and East Asian region, but weaken it over the Western Hemisphere in general. Significant change in spatial distribution from MU0 to MU1 is also found over the equatorial Indian Ocean. The MU plays a crucial role in forming the Indian Ocean Dipole, an east-west seesaw SST pattern along the equatorial Indian Ocean that is mainly matured during SON. It is also noted that the IM and EAM have different signs of variability of equinox asymmetry while they have the same sign for solstitial asymmetry in MU1. The first PC of the equinox asymmetry variability is also highly correlated with the Niño 3.4 SST index (Fig. 13b). MU0 has the highest correlation with the Niño 3.4 SST index during the preceding winter. However, in MU1, the first PC tends to concur with or slightly lead ENSO.

This section demonstrates that the MU strongly modulates the ENSO-monsoon relationship on interannual timescale. However, mechanisms for the modulation of this relationship and the influence of global monsoon change on ENSO change need further investigation.

7. Summary and Discussion

In this study, we explore the effect of the tectonic MU during the middle and late Cenozoic on the global monsoon system in terms of its spatial distribution, annual cycle, amplitude, and relationship with ENSO using MRI-CGCM experiments with progressive MU varying from 0 to 1.4 times the height of the present-day mountains. Land-sea distribution is preserved for all experiments and all mountains in the world were varied uniformly. The control run (MU1) reflects the present-day MU and the no-mountain run (MU0) uses a realistic land-sea distribution, but with a zero height for all mountains.

The comparison between MU0 and MU1 results reveals significant changes in the annual and seasonal means of precipitation, atmospheric circulation, and SST over the regions not only proximal to but also remote from the uplifted terrains (Figs. 1-2). Above all, the A-AM system exhibits drastic changes with the MU in all seasons. The annual mean precipitation averaged over the A-AM region and that over the Americas increase by about 16% and 9%, respectively, from MU0 to MU1, while that over Africa decreases by about 10%. The annual mean precipitation over the entire globe remains the same (Fig. 3). Notably, the MU's effect during transition seasons is as prominent as that during solstice seasons. The MU plays an essential role in shaping pre-monsoon circulation in MAM and thus advancing the seasonal march and summer-monsoon onset, especially in the Northern Hemisphere.

By analyzing the AC of regional precipitation with the progressive MU in eight monsoon sub-domains in the observation and the coupled experiments, it is shown that the MU plays a significant role in determining the phase and amplitude of the precipitation AC in regional sub-monsoon domains, particularly over the four regional components of the A-AM system. The EAM is the most sensitive to the progressive MU and cannot be established without the MU, while other regional monsoon systems can (Fig. 4). The amount of summer mean precipitation over the EAM region increases by 74% and the amplitude of the annual cycle is enhanced by 50% from MU0 to MU1. In general, the progressive MU considerably advances timing of summer-monsoon onset but has a relatively small effect on monsoon retreat, resulting in lengthening of the rainy period in most of the sub-monsoon domains.

The advance of seasonal march in the EAM and WNPM regions is attributed to significant intensification of the North Pacific anticyclonic circulation (Fig. 2a), prompting pre-monsoonal precipitation (Fig. 1a) with the MU during spring. In the IM region, the advance of seasonal march in SST seems to be partly responsible for pre-monsoonal precipitation. The observed climatology results show a strong SST warming in the equatorial Indian Ocean around March, which is continuously shifted northward with time (not shown). Without the MU, the northward propagation of the SST-warming is delayed by about two months and occurs rather discontinuously. Progressive MU continuously accelerates the seasonal march of SST, and MU1 realistically reproduces it despite the systematic warm bias.

With the aim of understanding the role of the MU on the global monsoon system, a series of coupled experiments with the progressive MU is evaluated in terms of the three-parameter metrics for delineating the primary climatological features of the global monsoon that includes the solstice monsoon mode, the equinox asymmetric mode, and monsoon rain domains (Wang and Ding, 2008). The analysis reveals that the solstice monsoon mode (the first AC mode) and monsoon rain domains are less sensitive to the progressive MU than the equinox asymmetric mode (the second AC mode) (Figs. 6, 8, and 10). Interestingly, the global monsoon does exist without the mountains, but the most realistic distribution is found in the experiment with a MU of 0.8 times the height of the present-day elevation (Figs. 10). The spring-fall asymmetry mode tends to prevail over the global tropics without the MU, and the progressive MU considerably decreases the asymmetry over the Western Hemisphere and the Indian Ocean in particular. Because of the significant systematic error in MU1, the exaggerated MU tends to help the model to reproduce the second AC mode more accurately.

It is also noted that the MU strongly modulates interannual variation in global monsoon precipitation in relation to ENSO. Progressive MU changes not only spatial distribution but also periodicity of the leading EOF mode of the first and second AC mode. The time variation in the EOF mode in MU1 is shorter and less periodic than that in MU0 in relation to

changes in ENSO characteristics. In MU0, ENSO and its association with global monsoon tend to have 4- to 5-year periodicity while they tend to have 2- to 3-year periodicity in MU1. The MU modulation on ENSO-monsoon relationship needs further investigation.

The MRI-CGCM using the realistic MU parameters is capable of reproducing the global precipitation climatology, but it also exhibits systematic bias due to model physics and the lack of realistic treatment of the narrow mountain ranges. Given the fact that MU0.8 has the best skill in capturing the solstice monsoon mode (not shown) and monsoon rain domain (Fig. 10), the model's systematic bias may vitiate the interpretation of the experiments with the progressive MU. Improvement of model physics for better representation of precipitation and SST climatology may be necessary for future study. In particular, the systematic bias in simulating the EASM and WNPM precipitation that is one of the common biases in the current CGCMs (Lee et al., 2010, 2014) should be improved. As indicated in Kitoh (2010), the horizontal resolution of the model used in this study is rather coarse (about 280 km) and is not sufficient to resolve the realistic land-sea distribution, topography, and steep mountains, particularly the Himalaya Ranges, Burmese Mountains, and so on. Coupled experiments using high-resolution GCM will be needed for better understanding.

Acknowledgments. This work was funded by the Korea Meteorological Administration Research and Development Program under Grant KMIPA 2015-2113 and the Korean government (MEST) National Research Foundation of Korea (NRF) grant (No. 2012R1A2A2A01008501). This is the ESMC publication number 62. We would like to thank the two reviewers for their helpful comments and suggestions, which improved the manuscript.

Edited by: Huang-Hsiung Hsu

REFERENCES

Abe, M., A. Kitoh, and T. Yasunari, 2003: An evolution of the Asian summer monsoon associated with mountain uplift-simulation with the MRI atmosphere-ocean coupled GCM. *J. Meteor. Soc. Japan,* **71**, 909-933.

Abe, M., T. Yasunari, and A. Kitoh, 2004: Effects of large-scale orography on the coupled atmosphere-ocean system in the tropical Indian and Pacific Oceans in boreal summer. *J. Meteor. Soc. Japan,* **82**, 745-759.

_____, _____, and _____, 2005: Sensitivity of the central Asian climate to uplift of the Tibetan Plateau in the coupled climate model (MRI-CGCM1). *Isl. Arc,* **14**, 378-388.

Barron, E. J., 1985: Explanations of the tertiary global cooling trend. *Palaeogeogr. Palaeocl.,* **50**, 45-61.

_____, C. G. A. Harrison, J. L. Sloan III, and W. W. Hay, 1981: 1980 million years ago to the present. *Paleogeography,* **74**, 443-470.

Boos, W. R., and Z. Kuang, 2010: Dominant control of the South Asian monsoon by orographic insulation versus plateau heating. *Nature,* **463**, 218-222.

Broccoli, A. J., and S. Manabe, 1992: The effects of orography on midlatitude North Hemisphere dry climates. *J. Climate,* **5**, 1181-1201.

Chang, C. P., Z. Wang, J. McBride, and C. H. Liu, 2005: AC of Southeast Asia-Maritime continent rainfall and the asymmetric monsoon transition. *J. Climate,* **18**, 287-301.

Hanh, D. G., and S. Manabe, 1975: The role of mountains in the south Asian monsoon circulation. *J. Atmos. Soc.,* **32**, 1515-1541.

Jiang D., Z. Ding, H. Drange, and Y. Gao, 2008: Sensitivity of East Asian climate to the progressive uplift and expansion of the Tibetan Plateau under the Mid-Pliocene boundary condition. *Adv. Atmos. Sci.,* **25**, 709-722.

Kim, H.-J., and Coauthors, 2011: Global monsoon, El Niño, and their interannual linkage simulated by MIROC5 and the CMIP3 CGCMs. *J. Climate,* **24**, 5604-5618.

Kitoh, A., 1997: Mountain uplift and surface temperature changes. *Geophys. Res. Lett*., **24**, 185-188.

_____, 2002: Effects of large-scale mountains on surface climate-a coupled ocean-atmospheric general circulation model study. *J. Meteor. Soc. Japan,* **80**, 1165-1181.

_____, 2004: Effects of mountain uplift on East Asian summer climate investigated by a coupled atmosphere-ocean GCM. *J. Climate,* **17**, 783-802.

_____, 2007: ENSO modulation by mountain uplift. *Clim. Dynam.,* **28**, 781-796.

_____, T. Motoi, and O. Arakawa, 2010: Climate modeling study on mountain uplift and Asian monsoon evolution. In: P. D. Clift, R. Tada, and H. Zheng (eds) *Monsoon Evolution and Tectonics-Climate Linkage in Asia,* 293-301.

Kutzbach, J. E., P. J. Guetter, W. F. Ruddiman, and W. L. Prell, 1989: Sensitivity of climate to late Cenozoic uplift in southern Asia and the American West: Numerical experiment. *J. Geophys. Res.,* **94**, 18393-18407.

Lau, K. M., and P. H. Chan, 1983: Short-term climate variability and atmospheric teleconnections from satellite-observed outgoing longwave radiation. Part II: lagged correlations. *J. Atmos. Sci.,* **40**, 2751-2767.

Lee, J.-Y., and B. Wang, 2014: Future change of global monsoon in the CMIP5. *Clim. Dynam*., **42**, 101-119.

_____, _____, K.-H. Seo, J.-S. Kug, Y.-S. Choi, Y. Kosaka, and K.-J. Ha, 2014: Future change of Northern Hemisphere summer tropical-extratropical teleconnection in CMIP5 models. *J. Climate*, **27**, 3643-3664.

_____, and Coauthors, 2010: How are seasonal prediction skills related to models' performance on mean state and annual cycle?. *Clim. Dynam.,* **35**, 267-283.

Lee, S.-S., J.-Y. Lee, K.-J. Ha, B. Wang, A. Kitoh, Y. Kajikawa, and M. Abe, 2013: Role of Tibetan Plateau on climatological annual variation of mean atmospheric circulation and storm track activity. *J. Climate,* **26**, 5270-5286.

Liu, J., B. Wang, Q. Ding, X. Kuang, W. Soon, and E. Zorita 2009: Centennial variations of the global monsoon precipitation in the last millennium: results from ECHO-G model. *J. Climate,* **22**, 2356-2371.

_____, _____, S.-Y. Yim, J.-Y. Lee, J.-G. Jhun, and K.-J. Ha, 2012: What drives the global summer monsoon over the past millennium?. *Clim. Dynam.* **39**, 1063-1072.

Liu, X., and Z. Y. Yin, 2002: Sensitivity of East Asian monsoon climate to the uplift of the Tibetan Plateau. *Palaeogeogr. Palaeocl.,* **183**, 223-245.

Manabe, S., and T. B. Terpstra, 1974: The effects of mountains on the general circulation of the atmosphere as identified by numerical experiments. *J. Atmos. Sci.,* **31**, 3-42.

Meehl, G. A., 1987: The annual cycle and interannual variability in the tropical Pacific and Indian Ocean regions. *Mon. Wea. Rev.,* **115**, 27-50.

Okajima, H., and S. P. Xie, 2007: Orographic effects on the northwestern Pacific monsoon: role of air-sea interaction. *Geophys. Res. Lett*., **34**, L21708, doi:10.1090/2007GL032206.

Ose, T., 1998: Seasonal change of Asian summer monsoon circulation and

its heat source. *J. Meteor. Soc. Japan,* **76**, 1045-1063.

Park, H.-S., S.-P. Xie, and S.-W. Son, 2013: Poleward stationary eddy heat transport by the Tibetan Plateau and equatorward shift of westerlies during Northern winter. *J. Atmos. Sci*., **70**, 3288-3301.

Ruddiman, W. F., and M. E. Raymo, 1988: Northern Hemisphere climate regimes during the past 3 Ma: Possible tectonic connections. *Philos. T. R. Soc. Lond. Ser. B,* **318**, 411-430.

_____, and J. E. Kutzbach, 1989: Forcing of late Cenozoic Northern Hemisphere climate by plateau uplift in southern Asia and the American West. *J. Geophys. Res.,* **94**, 18409-18427.

Sepulchre, P., G. Ramstein, F. Fluteau, M. Schuster, J. J. Tiercelin, and M. Brunet, 2006: Tectonic uplift and eastern Africa aridification. *Science,* **313**, 1419-1423.

Smith, T. M., and R. W. Reynolds, 2004: Improved extended reconstruction of SST (1854-1997). *J. Climate,* **17**, 2466-2477.

Su, F., X. Duan, D. Chen, Z. Hao, and L. Cuo, 2013: Evaluation of the global climate models in the CMIP5 over the Tibetan Plateau. *J. Climate*, **26**, 3187-3208.

Trenberth, K. E., and D. P. Stepaniak, 2004: The flow of energy through the earth's climate system. *Quart. J. Roy. Meteor. Soc.,* **130**, Part B, 2677-2701.

_____, _____, and J. M. Caron, 2000: The global monsoon as seen through the divergent atmospheric circulation. *J. Climate,* **13**, 3969-3993.

_____, J. W. Hurrell, and D. P. Stepaniak, 2006: *The Asian Monsoon.* The Asian monsoon: Global perspectives, Springer, 67-87.

Wang, B., and Q. Ding, 2008: The global monsoon: Major modes of annual variation in tropical precipitation and circulation. *Dyn. Atmos. Oceans,* **44**, 65-183.

_____, H.-J. Kim, K. Kikuchi, and A. Kitoh, 2011: Diagnostic metrics for evaluation of annual and diurnal cycles. *Clim. Dynam.,* **37**, 941-955.

_____, J. Liu, H.-J. Kim, P. J. Webster, and S.-Y. Yim, 2012: Recent change of the global monsoon precipitation (1979-2008). *Clim. Dynam.*, **39**, 1123-1135.

Webster, P. J., V. O. Magana, T. N. Palmer, J. Shukla, R. A. Tomas, M. Yanai, and T. Yasunari, 1998: Monsoon: processes, predictability, and the prospects for prediction. *J. Geophys. Res.,* **103**, 14451-14510.

Wu, G., and Coauthors, 2007: The influence of mechanical and thermal forcing by the Tibetan Plateau on Asian climate. *J. Hydrometeor.,* **8**, 770-789.

Xie, P., and P. A. Arkin, 1997: Global precipitation: A 17-year monthly analysis based on gauge observations, satellite estimates, and numerical model outputs. *Bull. Amer. Meteor. Soc*., **78**, 2539-2558.

Yasunari, T., K. Saito, and K. Takata, 2006: Relative roles of large-scale orography and land surface processes in the global hydroclimate. Part I: impacts on monsoon systems and the tropics. *J. Hydrometeor.,* **7**, 626-641.

Yukimoto, S., and Coauthors, 2001: The new Meteorological Research Institute coupled GCM (MRI-CGCM2)-model climate and variability. *Pap. Meteorol. Geophys.,* **51**, 47-88.